Polym. Korea, Vol. 50, No. 2, pp. 210-219 (2026)
https://doi.org/10.7317/pk.2026.50.2.210
ISSN 2234-8077(Online)

착용형 열 관리를 위한 형태 안정성 에폭시-PCM 코팅 나일론 직물

이재경*·김민수*·김주헌*,**,†

*중앙대학교 화학공학과, **중앙대학교 대학원 지능형에너지산업융합학과

(2025년 7월 22일 접수, 2025년 10월 14일 수정, 2025년 10월 29일 채택)

Shape-Stable Epoxy-PCM Coated Nylon Fabrics for Wearable Thermal Management

Jaekyung Lee*, Minsu Kim*, and Jooheon Kim*,,†**

**School of Chemical Engineering, Chung-Ang University, Seoul 06974, Korea*
***Department of Intelligent Energy and Industry, Graduate School, Chung-Ang University, Seoul 06974, Korea*

(Received July 22, 2025; Revised October 14, 2025; Accepted October 29, 2025)

초록: 본 연구는 에폭시 말단 디메틸실록산(KF-105, EP) 매트릭스에 라우르산(LA)과 미리스트산(MA)을 화학적으로 그래프트한 형태 안정성 상변화물질(PCM) 복합체를 제조하고, 이를 나일론 직물에 코팅하여 고급 열 조절 텍스타일을 개발한 연구이다. 화학적 그래프팅 전략을 통해 LA와 MA를 EP 네트워크에 공유결합으로 결합시켰으며, FTIR 분광법과 FE-SEM을 통해 상분리 없는 균질하고 통합된 형태학을 확인했다. DSC 분석 결과, 화학적으로 통합된 LMEP 복합체는 22-40 °C의 넓은 상전이 온도 범위에서 약 82.1 J/g의 상당한 잠열을 보여 효과적인 열에너지 저장 능력을 나타냈다. LMEP 복합체는 순수 PCM 대비 인장강도가 약 9배, 파단 연신율이 40배 향상된 우수한 기계적 특성을 보였다. 매트릭스 내 견고한 공유결합으로 인해 융점보다 훨씬 높은 온도에서도 형태 안정성과 PCM 누출 방지 성능이 탁월했다. 나일론 직물에 코팅된 NF/LMEP 복합체는 41.2 J/g의 잠열을 유지했으며, 150회 열순환 후에도 잠열이 3.4%만 감소하는 뛰어난 장기 열순환 안정성을 보였다. IR 열화상 분석을 통해 NF/LMEP 복합체가 순수 나일론 대비 온도 전달을 효과적으로 지연시키고 낮은 표면온도를 유지하는 우수한 열 조절 성능을 확인했다. 이러한 결과는 PCM의 에폭시 매트릭스 화학적 통합이 지속적인 편안함과 안정성을 요구하는 차세대 웨어러블 열 조절 응용 분야 개발을 위한 매우 유망한 접근법임을 보여준다.

Abstract: This study presents shape-stable phase change material (PCM) composites by chemically grafting lauric acid (LA) and myristic acid (MA) into an epoxy-terminated dimethylsiloxane matrix and coating onto nylon fabric for thermal regulation textiles. The chemically integrated LA-MA epoxy composite (LMEP) exhibited broad phase transition from 22-40 °C with substantial latent heat of 82.1 J/g. Mechanical properties were significantly enhanced with 9-fold increase in tensile strength and 40-fold increase in elongation compared to pristine PCMs. The composite showed excellent shape stability and negligible PCM leakage due to robust covalent bonding. The LMEP-coated nylon fabric (NF/LMEP) maintained 41.2 J/g latent heat and demonstrated excellent thermal cycling stability with only 3.4% decrease after 150 cycles. IR thermography confirmed superior thermal regulation performance, effectively delaying temperature transmission compared to bare nylon fabric. These findings demonstrate that chemical integration of PCMs into epoxy matrices offers a promising approach for next-generation wearable thermal regulation applications.

Keywords: polymer-matrix composites, phase-change materials (PCMs), textile, latent heat, thermal management.

Introduction

Smart textiles mark a transformative leap in wearable technologies by embedding functions such as self-monitoring, adaptability, and autonomous repair directly into fabrics. These cutting-edge materials are central to applications like bendable displays, wearable electronics, protective clothing, and flexible energy systems. Recently, there has been a growing focus on developing textiles capable of multifunctional responses to environmental stimuli while maintaining thermal comfort for the wearer.[1-3] A core requirement in this field is the development of fibers

†To whom correspondence should be addressed.
Jooheonkim@cau.ac.kr, ORCID 0000-0002-6644-7791
©2026 The Polymer Society of Korea. All rights reserved.

that can promptly react to various external cues. These functional fibers are integral to the realization of wearable platforms that combine user comfort with high responsiveness. Nevertheless, producing such fibers remains technically demanding due to the stringent environmental conditions involved in their fabrication.[4,5]

The need for smart textiles is especially urgent in occupations that involve exposure to extreme heat and humidity, such as those of nucleic acid sampling personnel, miners, kiln workers, metallurgists, and firefighters. Extended exposure in these settings often leads to critical heat accumulation around the body, disrupting the thermal equilibrium and posing risks of heat-related illnesses. Without proper thermal regulation, these conditions can endanger workers' health and impair operational efficiency. The application of smart textile technology presents a promising solution by enabling garments that actively regulate both temperature and humidity, thus enhancing safety and productivity in challenging work environments. The advancement of fiber engineering techniques capable of endowing garments with real-time thermal responsiveness is key to realizing intelligent clothing for such demanding applications.

Organic phase change materials (PCMs), including paraffin,[6] stearic acid,[7] and palmitic acid,[8] are known for their capacity to absorb and release substantial amounts of thermal energy through solid–liquid transitions.[9-12] Unlike conventional heat-conductive materials, PCMs utilize latent heat during phase transformation, enabling efficient thermal storage and temperature regulation.[13-16] These materials undergo reversible phase changes within specific temperature ranges, allowing them to buffer thermal fluctuations by storing heat during excess and releasing it when temperatures drop. As such, organic PCMs are considered highly effective materials for thermal management across diverse applications.

Current research is focused on integrating PCMs into textile systems to develop thermally responsive garments.[17,18] Considerable efforts have been made to improve the synthesis, thermal characterization, and structural integration of organic PCMs with textile substrates, aiming to enhance performance and operational reliability. However, several technical barriers remain. These include achieving strong interfacial compatibility, improving mechanical durability, and ensuring thermal stability under repeated use. Such challenges are particularly critical for applications involving mechanical deformation, repeated heating and cooling, and potential environmental contamination.

One of the most pressing limitations of organic PCMs is their propensity to leak during phase transitions, which severely restricts their practical use.[19,20] A widely adopted strategy to mitigate this issue is to embed encapsulated PCM particles within textile matrices. The encapsulating shell helps prevent leakage, yet each capsule's interface with the surrounding fibers introduces thermal resistance and reduces the effective latent heat capacity of the system.[21] This fragmented energy storage and structural incompatibility can negatively impact on the overall thermal performance and reliability of PCM-loaded textiles.

To overcome these limitations, our study proposes a novel strategy involving the chemical integration of fatty acid-based PCMs into a polymer matrix, thereby achieving superior shape stability, enhanced mechanical properties, and durable thermal regulation capabilities. We specifically focus on chemically grafting lauric acid (LA) and myristic acid (MA) into an epoxy-terminated dimethylsiloxane (EP) oligomer to form a ternary composite (LMEP). This chemical bonding approach is designed to prevent PCM leakage intrinsically, circumventing the need for physical encapsulation and allowing for high PCM content without compromising structural integrity.[16] The synthesized LMEP composite is then seamlessly coated onto nylon fabric (NF) to create functional thermal regulation textiles suitable for wearable applications. This paper systematically investigates the chemical structure, morphology, thermal phase change behavior, mechanical properties, and shape stability of the synthesized EP–PCM composites. Crucially, the long-term thermal cycling stability and the practical thermal regulation performance of the NF/LMEP textile are comprehensively evaluated using infrared (IR) thermography in direct skin contact. Our findings demonstrate that the chemical grafting strategy effectively addresses the critical challenges of PCM leakage and stability, positioning the developed NF/LMEP composite as a highly promising candidate for next-generation smart textiles demanding prolonged thermal comfort and robust performance.

Experimental

Materials. Hexamethylenetetramine, LA, and MA were procured from Sigma-Aldrich and utilized as received. The epoxy-terminated dimethylsiloxane (ETDS) oligomer, designated as KF-105 (EP) and characterized by an equivalent weight of 490 g/eq and a density of 0.99 g/cm^3, was obtained from Shin-Etsu Chemical Co., Ltd. The nylon fiber (NF) fabric was obtained from RTBIO (Bucheon, Korea).

Fabrication of PCM Coated NF. To prepare the composite coatings, 3 g of KF-105 was mixed with 1 g of hexamethylenetetramine as a curing agent and stirred at room temperature

for 10 min until a transparent solution was formed. Subsequently, 4 g of molten PCMs (LA, MA, or 3:1 LA/MA (by weight)) were separately added to three such solutions, corresponding to a PCM-to-epoxy weight ratio of 4:3. Each mixture was then reacted on a hotplate at 150 ℃ for 10 min. The resulting products are referred to hereafter as the LAEP, MAEP, and LMEP, respectively. After cooling to room temperature and reaching a viscosity that allowed smooth and uniform brush application without excessive flow or dripping, each formulation was evenly applied onto NF substrates using a rubber brush. The coated fabrics were cured in an oven at 120 ℃ for 15 min and then air-dried to obtain the final NF/LAEP, NF/MAEP, and NF/LMEP samples.

Characterization. Fourier transform infrared spectroscopy (FTIR, Perkin-Elmer Spectrum One, USA) in attenuated total reflectance (ATR) mode was utilized to identify chemical structural changes induced by surface treatment. The morphology of the composites was analyzed using field-emission scanning electron microscopy (FE-SEM, SIGMA 300, Carl Zeiss, Germany). Thermal diffusivity (α, mm^2/s) was measured using a laser flash analyzer (LFA 1000, Linseis, Germany), while both the specific heat capacity (C_p, J/g·K) and latent heat (ΔH, J/g) were determined using a differential scanning calorimeter (DSC-7, Perkin-Elmer Co., USA). Thermal conductivity (K, W/m·K) was subsequently calculated using the equation $K = \alpha \times C_p \times \rho$, where ρ (g/cm^3) represents the bulk density of the composites. Mechanical properties were evaluated with a universal testing machine (UTM, model 3344Q9465, Instron Co., USA) at a crosshead speed of 2 mm/min according to ASTM D638 standards. Thermal degradation behavior was assessed by thermogravimetric analysis (TGA-2050, TA Instruments, USA), wherein samples were heated from room temperature to 600 ℃ at a rate of 10 ℃/min under a nitrogen atmosphere.

Results and Discussion

The fabrication process of the LMEP matrix and its subsequent coating onto the NF substrate is shown schematically in Figure 1. Initially, LA and MA were incorporated into the EP matrix through epoxy ring-opening reactions using hexamethylenetetramine as a curing agent, followed by esterification between the carboxylic acid groups of PCMs and the opened epoxy moieties. This chemical reaction ensures the effective covalent integration of PCM segments into the EP network, thereby addressing the poor interfacial compatibility observed in conventional PCM-epoxy systems. Following LMEP synthesis, the formulation was cooled to a suitable viscosity, evenly

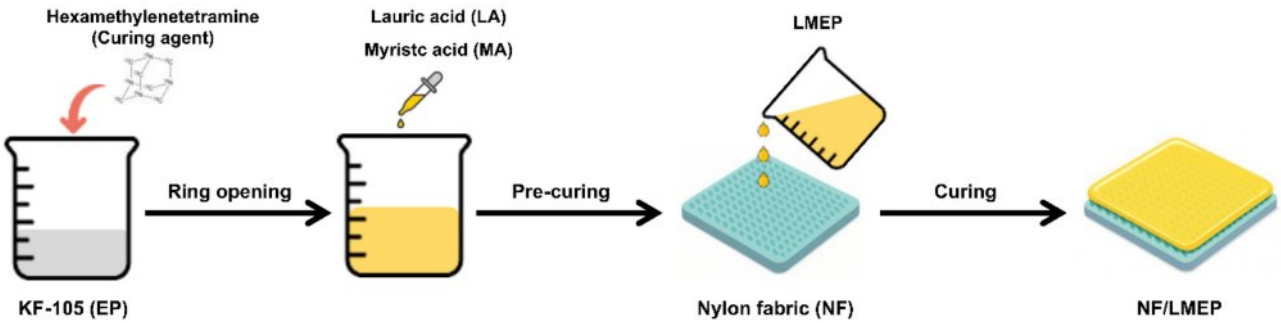

Figure 1. Schematic diagram showing the fabrication process of the LMEP matrix and its subsequent coating onto the NF substrate.

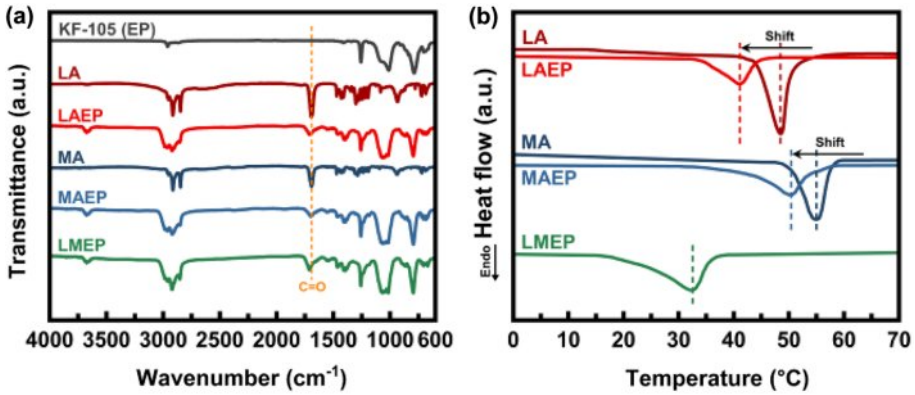

Figure 2. (a) FTIR spectra; (b) DSC analyses of the starting materials and various composites.

applied onto NF substrates using a rubber brush, and subsequently cured to obtain the final NF/LMEP composite. This comprehensive approach results in a chemically integrated structure with enhanced stability and robust thermal energy storage capability.

The chemical structures and bonding states of the pristine components—KF-105(EP), LA, and MA—as well as the synthesized binary composites (LAEP and MAEP) and ternary composite (LMEP), were characterized by FT-IR spectroscopy (Figure 2(a)). The unreacted EP exhibited a characteristic peak at 911 cm^{-1}, corresponding to the asymmetric stretching vibration of the epoxy ring. Pristine LA and MA show strong C=O stretching vibrations at 1695 cm^{-1} and 1694 cm^{-1}, respectively, indicative of their carboxylic acid functional groups. Upon incorporation of LA and MA into the EP matrix, both LAEP and MAEP composites demonstrate distinct shifts of the carboxylic C=O peaks from their original positions at 1695 cm^{-1} and 1694 cm^{-1} to ester carbonyl bands at approximately 1710 cm^{-1} and 1705 cm^{-1}, respectively. These spectroscopic changes, accompanied by significant reductions in the epoxy peak intensity at 911 cm^{-1}, provide compelling evidence for successful ester bond formation through ring-opening reactions between the carboxylic acid groups of the fatty acids and the epoxy moieties. The LMEP sample exhibited a comprehensive spectral profile encompassing features from both LAEP and MAEP, including a prominent ester C=O stretching band at approximately 1713 cm^{-1} and the almost complete disappearance of the epoxy peak at 911 cm^{-1}. This spectral evolution confirmed the successful dual esterification of EP with both LA and MA, thereby demonstrating the covalent integration of both fatty acid chains into the EP network. These findings indicate that the ternary system underwent efficient ring-opening and ester-forming reactions, leading to a chemically integrated PCM structure with enhanced thermal and structural stability.

The thermal behaviors of pristine components and their epoxy-based composites were thoroughly investigated by differential scanning calorimetry (DSC), with the results depicted in Figure 2(b). A comprehensive summary of their key thermal parameters, including melting points and latent heats, is provided in Table 1. The melting points were consistently determined from the maximum endothermic peak temperature. The pristine LA and MA exhibited sharp, distinct melting transitions at approximately 48.5 ℃ and 55.0 ℃, respectively, characteristic of their highly ordered intrinsic crystalline phase change behaviors. It is noteworthy that the EP oligomer does not display any significant endothermic peak within the examined temperature range in Figure 2(b), signifying its thermal inertness with respect to phase changes.

Table 1. Melting Points and Latent Heat Values of Pristine PCMs and Their Epoxy-based Composites

Material	Melting point (°C)	Latent heat (J/g)
LA	48.5	198.4
MA	55.0	187.3
LAEP	41.1	71.6
MAEP	50.2	85.3
LMEP	32.4	82.1

After the incorporation of LA and/or MA into the EP matrix, substantial alterations in the thermal properties were observed for the resultant composites. The LAEP sample displayed a melting temperature of 41.1 ℃ while the MAEP sample exhibited a melting temperature of 50.2 ℃. Both composites showed notable reductions in their melting temperatures compared to their pristine counterparts. This reduction in melting temperature is primarily attributed to the esterification process occurring between the carboxyl groups of LA or MA and the EP moiety. This chemical bonding consumes carboxylic acid groups, thereby disrupting the extensive intermolecular hydrogen bonding network characteristic of pristine fatty acids. The resultant decrease in hydrogen bonding and disruption of crystalline order directly led to a notable reduction in crystallinity and, consequently, a lower melting temperature.

In distinct contrast to the relatively sharp, single transitions observed for LAEP and MAEP, the LMEP composite exhibited a broad endothermic transition spanning from 22 to 40 ℃, with a primary peak at 32.4 ℃, notably lacking any distinct multiple peaks. This broadened transition and lower peak temperature for LMEP are primarily attributed to the formation of a highly disordered and homogeneously crosslinked network. The simultaneous covalent incorporation of two different PCM segments (LA and MA) into the rigid epoxy backbone significantly increases the structural heterogeneity, creating a more amorphous structure that hinders the formation of well-ordered crystalline domains. This synergistic effect of enhanced structural heterogeneity and disrupted long-range order results in a broader and lower-temperature phase transition. This broad temperature range (22 to 40 ℃) is particularly advantageous, as it closely aligns with the human skin temperature range (typically 32–35 ℃, varying with activity and environment), making LMEP an exceptionally suitable PCM for wearable thermal regulation applications aimed at maintaining physiological comfort. Nevertheless, despite its reduced crystallinity, the LMEP maintained a substantial latent heat of approximately 82.1 J/g, indicating the

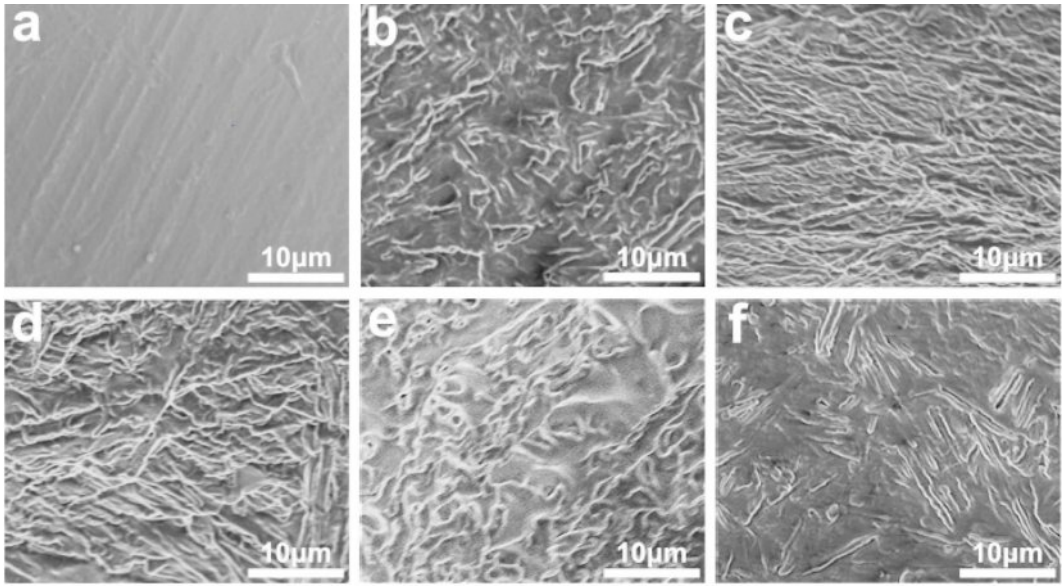

Figure 3. FE-SEM images of (a) the pristine KF-105 (EP); (b) the pure LA; (c) the pure MA; (d) the LAEP; (e) the MAEP; (f) the LMEP.

successful retention of significant phase change enthalpy within the chemically integrated structure. This result robustly confirmed the effective integration of both PCM species into the EP matrix and supports the formation of a structurally disordered, yet highly efficient, thermally active dual-component system.

The morphological evolution of the epoxy–PCM composites, providing crucial insights into their structural integrity and component distribution, was comprehensively revealed by field-emission scanning electron microscopy (FE-SEM) images presented in Figure 3. Specifically, the pristine EP oligomer (Figure 3(a)) exhibited a relatively smooth and dense morphology, consistently devoid of discernible phase domains, which agrees with its homogeneous oligomeric nature. In stark contrast, pure LA (Figure 3(b)) displayed a typical crystalline structure characterized by prominent, well-defined facets, reflecting its highly ordered solid state. Similarly, MA (Figure 3(c)) also presented a distinct crystalline morphology, aligning precisely with its nature as fatty acid.

Following esterification, all synthesized composites–LAEP (Figure 3(d)), MAEP (Figure 3(e)), and LMEP (Figure 39f))–exhibited remarkably uniform and integrated morphologies. Crucially, these composites were distinctly different from their pristine, individual components and completely devoid of any observable macroscopic phase separation, a critical indicator of successful material integration. This observed homogeneous microstructure across all composites directly confirmed the successful formation of chemically bonded networks through esterification, thereby unequivocally signifying the effective covalent incorporation of LA, MA, or both, into the EP matrix. The absence of any segregated PCM domains further underscores the robustness of this chemical integration. These observed morphological changes are highly consistent with the FTIR and DSC results, collectively demonstrating the paramount importance of successful chemical bonding, achieved through carefully controlled reaction parameters, in realizing well-defined, morphologically stable, and integrated composite architectures with improved structural stability and performance.

To comprehensively characterize the performance of the EP–PCM composites, their thermal and mechanical properties were rigorously evaluated, as illustrated in Figure 4. Specifically, Figure 4(a) presents the thermal conductivity and latent heat values for EP, LAEP, MAEP, and LMEP. A notable observation was the increase in TC for LAEP, MAEP, and LMEP compared to pristine EP. This enhancement is attributed to the intrinsically higher thermal conductivity of the incorporated PCMs (LA and MA), and these composites consistently exhibited a substantial latent heat of approximately 80 J/g, reinforcing their significant thermal energy storage capacity for practical applications.

The mechanical integrity of the synthesized composites is of critical importance for their practical applications. Figure 4(b) illustrates the representative tensile stress-strain curves for the pristine EP and various PCM-EP composites. These curves distinctly showed that all PCM-EP composites exhibited a clear enhancement in mechanical properties compared to the pristine PCMs. Further quantitative assessment of the mechanical per-

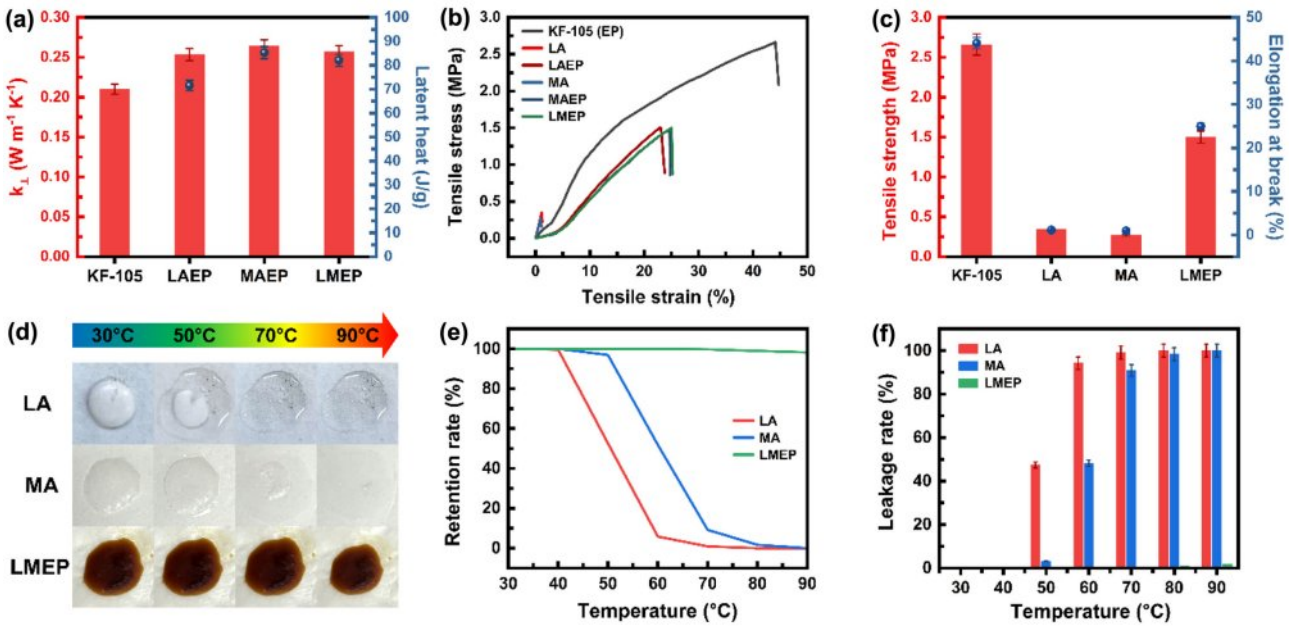

Figure 4. Comprehensive characterization of EP–PCM composites: (a) thermal conductivity and latent heat values; (b, c) mechanical properties; (d) photo of the leakage test process; (e) retention rate; (f) leakage rate.

formance, particularly for LMEP, was provided in Figure 4(c). This bar graph distinctively presents the tensile strength and elongation at break of LMEP, offering a clear quantitative representation of its enhanced mechanical properties. Notably, as confirmed by this quantitative data, LMEP demonstrated significant improvements, with its tensile strength and elongation at break enhanced by approximately 9-fold and 40-fold, respectively, when compared to the pristine LA and MA. These findings underscore the robust mechanical reinforcement achieved through the chemical integration of PCMs into the epoxy matrix.

Beyond thermal and mechanical properties, the shape stability and PCM retention are critical for practical applications, particularly when composites are subjected to temperatures above the PCM melting points. For a quantitative evaluation of the leakage behavior, the retention rate (ϵ) and leakage rate (γ) of the samples were calculated. These parameters provide a precise measure of PCM confinement and loss, respectively, and are defined by the following equations:

$$\varepsilon = \frac{m_r}{m_0} \times 100\% \quad (1)$$

$$\gamma = \frac{m_0 - m_r}{m_0} \times 100\% \quad (2)$$

Here, m_0 denotes the initial mass of the PCM sample, while m_r represents the measured mass of the sample after a specific thermal treatment. Leakage tests were performed, with results presented in Figure 4(d)–(f). These figures illustrate that the introduction of epoxy enables the developed epoxy–PCM composites to prevent PCM leakage even when the materials are in their molten state. Notably, the measurements were conducted from 30 ℃ to 90 ℃, holding for 30 minutes at each 10 ℃ increment. In stark contrast, pristine LA (48.5 ℃) and MA (55.0 ℃), upon reaching their respective melting points, rapidly lost structural integrity and exhibited significant leakage, as would be evident in the absence of chemical confinement. However, the chemically integrated systems, particularly LMEP (melting point 32.4 ℃), demonstrated exceptional shape stability even at 90 ℃, far beyond its melting transition. As shown in Figure 4(e) and Figure 4(f), LMEP exhibited very high retention rates and negligible leakage rates, confirming its robust performance. This robust performance unequivocally highlights the critical role of covalent bonding between the epoxy matrix and the PCMs in suppressing PCM diffusion and ensuring long-term thermal and structural stability.

Figure 5(a) and (b) present the morphology of the NF/LMEP composite through surface and cross-section FE-SEM images, respectively. These images clearly demonstrated that LMEP was effectively coated onto the NF substrate, forming a cohesive and continuous layer with an average LMEP thickness of approximately 130 μm over the 250 μm nylon fabric substrate. This uniform and robust coating is essential for maintaining the structural integrity and functionality of the resultant composite textile.

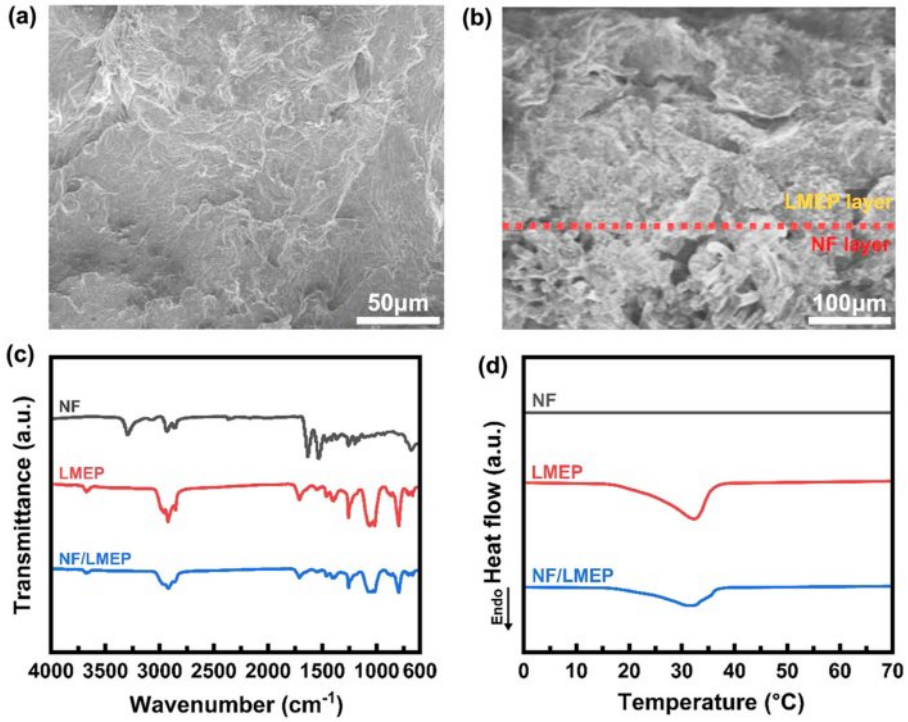

Figure 5. Comprehensive characterization of the NF/LMEP: (a, b) morphology from surface and cross-section FE-SEM images; (c) FTIR spectra; (d) DSC analysis.

Figure 5(c) presents the FT-IR spectra of NF, LMEP, and NF/LMEP. Notably, in the spectrum of NF/LMEP, the characteristic absorption peaks typically associated with the nylon fabric were not distinctly observed or were significantly attenuated. This phenomenon can be attributed to the comprehensive and uniform LMEP layer acting as an effective protective film, thereby hindering the infrared (IR) beam from fully penetrating and detecting the underlying nylon fibers. This observation directly confirmed that LMEP was thoroughly coated across the NF surface, indicating successful and complete coverage of the textile substrate. The thermal energy storage capabilities of the coated textile were assessed through DSC analysis, as presented in Figure 5(d). As expected, the pristine NF exhibited no significant heat flow peaks, confirming its thermal inertness regarding phase change. However, when LMEP was coated onto the nylon, the resulting NF/LMEP composite displayed a heat flow peak at a temperature nearly identical to that of bulk LMEP, with a similar peak shape. This confirmed that the phase change behavior of LMEP was well-preserved within the composite. Furthermore, the latent heat for NF/LMEP was measured to be 41.2 J/g, quantitatively demonstrating that the coated textile retains a substantial capacity for thermal energy storage.

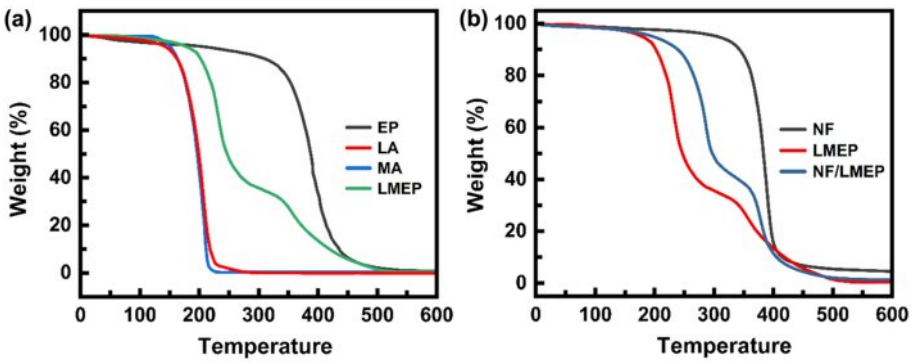

Figure 6. (a) TGA curves of pristine LA, MA, EP, and LMEP composite; (b) TGA curve of the NF/LMEP composite.

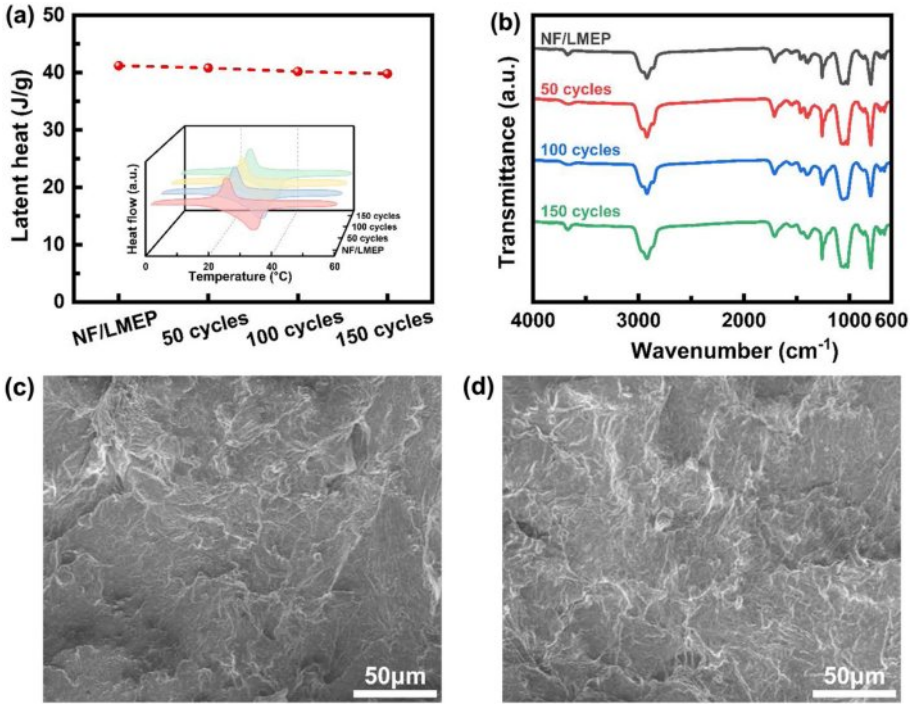

Figure 7. Long-term thermal cycling stability of NF/LMEP composite: (a) DSC curves after 50, 100, and 150 thermal cycles; (b) FTIR spectra assessing chemical stability after thermal cycling; (c, d) FE-SEM images revealing morphological stability before and after 150 thermal cycles.

As shown in Figure 6(a), the thermal degradation characteristics of the individual components offer crucial insights into the composite's behavior. Pristine LA and MA typically underwent thermal decomposition around 200 ℃. The EP matrix, on the other hand, exhibited its primary degradation stage at approximately 400 ℃. The LMEP composite, reflecting the thermal characteristics of its individual constituents, displayed a two-stage degradation profile. The initial decomposition occurring around 200 ℃ corresponded to the breakdown of the LA and MA components, while the second stage at approximately 400 ℃ was associated with the degradation of the epoxy matrix. This characteristic stepwise degradation pattern supports the successful integration of both PCM and epoxy components. Notably, LMEP exhibited significant thermal stability up to 200 ℃, indicating its inherent robustness in this temperature range. Figure 6(b) presents the TGA curve for the NF/LMEP composite, illustrating its thermal behavior when integrated into a textile. The degradation profile of NF/LMEP closely paralleled the thermal characteristics of its individual constituents. It exhibited an initial decomposition stage around 200 ℃, corresponding to the breakdown of the covalently bonded LA and MA components from LMEP. A second, more prominent degradation step was observed around 400 ℃, which was attributed to the combined decomposition of the epoxy matrix from LMEP and the NF substrate.

The long-term thermal cycling stability of the NF/LMEP composite is paramount for its practical application in thermal regulation textiles. This crucial stability was comprehensively evaluated through repeated DSC measurements, FTIR spectroscopy, and FE-SEM imaging after multiple thermal cycles, with the results presented in Figure 7. Figure 7(a) presents the DSC curves of NF/LMEP after 50, 100, and 150 thermal cycles. These results demonstrated the superior thermal reliability of the composite over extended use. Notably, after 150 consecutive cycles, only a minimal decrease in latent heat of approximately 3.4% was observed, indicating excellent retention of its thermal energy storage capacity. Importantly, the melting point of the composite remained unchanged throughout the entire cycling process, further confirming its robust thermal stability and consistent phase change performance over time.

To assess the chemical stability of NF/LMEP after repeated thermal cycling, FTIR spectroscopy was performed, as shown in Figure 7(b). By comparing the FTIR spectrum of the initial NF/LMEP composite with that after 150 thermal cycles, it was evident that the characteristic absorption bands remained consistent. The spectra exhibited highly similar features, indicating that the chemical structure of the composite remained unaltered and stable even after enduring extensive thermal cycles.

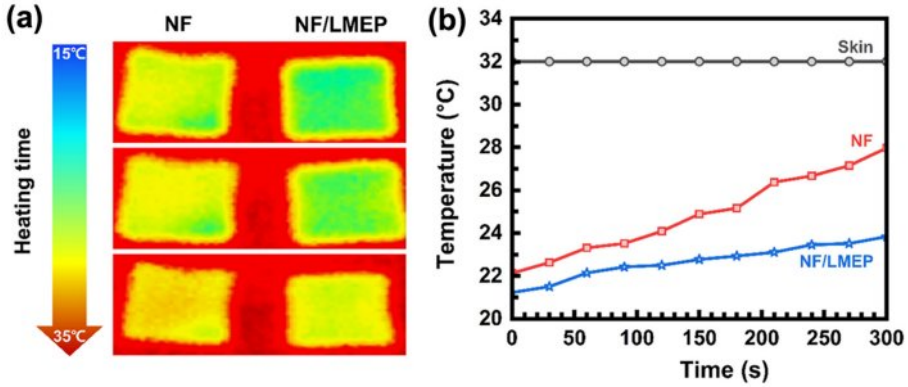

Figure 8. Infrared thermography analysis of thermal regulation performance: (a) IR thermal images of each sample captured at specific time points during direct skin contact; (b) dynamic surface temperature profiles of samples over a 300-second period.

The structural integrity and morphological stability of the NF/LMEP composite after cycling were verified by FE-SEM images. Figure 7(c) presents the surface morphology of the pristine NF/LMEP composite, while Figure 7(d) reveals the surface morphology of the composite after 150 thermal cycles. These comparative SEM images confirmed the exceptional structural stability of the NF/LMEP composite. No signs of leakage, cracking, or significant morphological degradation were observed, even after extensive thermal cycling. This demonstrated robustness and durability underscore the composite's suitability for practical applications that demand long-term stability and reliability in fluctuating temperature environments.

The thermal regulation performance of bare NF and the NF/LMEP composite was evaluated under direct skin contact for 300 seconds using IR thermography, as shown in Figure 8. IR thermal images in Figure 8(a) highlight the surface temperature evolution of each sample at selected time points. The bare NF exhibited a rapid increase in surface temperature, closely paralleling the skin temperature rise, due to its inability to absorb latent heat. In contrast, the NF/LMEP composite showed significantly slower thermal accumulation, maintaining the lowest surface temperature throughout the test. At the end of 300 seconds, the final surface temperatures of NF and NF/LMEP reached 32.84 ℃ and 27.97 ℃, respectively. While both samples initially exhibited a similar temperature rise up to around 22 ℃, the NF/LMEP composite showed a markedly reduced temperature increase once the phase change region was reached, indicating effective latent heat absorption and delayed thermal propagation. This superior performance stems from the synergistic incorporation of chemically grafted LA and MA into the epoxy matrix, which enabled an extended and more effective phase change region. Figure 8(b) presents the dynamic temperature curves, clearly demonstrating that the NF/LMEP composite effectively delayed heat transfer by absorbing thermal energy during the phase transition. These results confirm that epoxy-based PCM coatings substantially enhance the thermal buffering capability of textiles. In particular, the NF/LMEP composite offers outstanding heat absorption and sustained temperature suppression, making it a strong candidate for wearable thermoregulation applications requiring long-term comfort and thermal stability.

Conclusions

This study successfully developed a novel approach for fabricating highly stable and efficient epoxy-based PCM composites, LMEP, by chemically grafting LA and MA into an epoxy matrix, subsequently coated onto NF. Comprehensive characterization confirmed the successful chemical integration and homogeneous morphology of LMEP, which exhibited a broad phase transition (22–40 ℃) with a substantial latent heat of 82.1 J/g. This chemical approach significantly enhanced both mechanical strength and crucial shape stability, effectively preventing PCM leakage even above its melting point. When applied as coating, the NF/LMEP composite maintained robust thermal energy storage (41.2 J/g), demonstrating excellent long-term thermal cycling stability with minimal latent heat degradation after 150 cycles. Furthermore, IR thermography analyses conclusively showed the superior thermal buffering capability of the NF/LMEP textile, effectively delaying temperature transmission and maintaining a lower surface temperature. These findings collectively underscore the efficacy of the chemical grafting strategy in overcoming conventional PCM limitations, positioning the NF/LMEP composite as a highly promising and viable material for advanced wearable thermal regulation

applications demanding prolonged comfort and consistent performance.

Acknowledgments: This research was supported by the Chung-Ang University Research Scholarship Grants in 2024 and supported by the National Research Foundation of Korea (NRF) grant funded by the Korea government (MSIT) (RS-2024-00448445).

Conflict of Interest: The authors declare that there is no conflict of interest.

Supporting Information: Information is available regarding the materials used for preparing epoxy-PCM coated nylon fabrics, characterization techniques including FTIR, XPS, FE-SEM, thermal property measurements, mechanical testing, and electrical resistivity evaluation. The materials are available *via* the Internet at http://journal.polymer-korea.or.kr.

References

1. Orjuela-Garzón, I. C.; Rodríguez, C. F.; Cruz, J. C.; Briceño, J. C. Design, Characterization, and Evaluation of Textile Systems and Coatings for Sports Use: Applications in the Design of High-Thermal Comfort Wearables. *ACS Omega.* **2024**, 9, 49143-49162.
2. Jia, Z.; Cunha, S.; Aguiar, J. Study on Phase Change Materials Integration in Concrete: Form-stable PCM and Direct Addition. *Process Saf. Environ. Prot.* **2024**, 189, 1293-1302.
3. Orjuela-Garzón, I. C.; Rodríguez, C. F.; Cruz, J. C.; Briceño, J. C. Design, Characterization, and Evaluation of Textile Systems and Coatings for Sports Use: Applications in the Design of High-Thermal Comfort Wearables. *ACS Omega*. **2024**, 9, 49143-49162.
4. Wang, X.; Du, X.; Xu, D.; Wei, T.; Zhang, Q.; Chen, Z.; Kong, D.; Wei, K.; Zhou, L.; Zhu, B.; Xu, W.; Zhu, J. A Passive Sweat-Responsive Thermoregulatory Textile with the Largest Thermal Comfort Zone. *ACS Nano*. **2025**, 19, 19977-19988.
5. Fan, C.; Long, Z.; Zhang, Y.; Mensah, A.; He, H.; Wei, Q.; Lv, P. Robust Integration of Energy Harvesting with Daytime Radiative Cooling Enables Wearing Thermal Comfort Self-powered Electronic Devices. *Nano. Energy.* **2023**, 116, 108842.
6. Shen, Z.; Kwon, S.; Lee, H. L.; Toivakka, M.; Oh, K. Cellulose Nanofibril/carbon Nanotube Composite Foam-stabilized Paraffin Phase Change Material for Thermal Energy Storage and Conversion. *Carbohydr. Polym.* **2021**, 273, 118585.
7. Tan, Q.; Liu, H.; Shi, Y.; Zhang, M.; Yu, B.; Zhang, Y. Lauric Acid/stearic Acid/nano-particles Composite Phase Change Materials for Energy Storage in Buildings. *J. Energy. Storage.* **2024**, 76, 109664.
8. Dai, J.; Ma, F.; Fu, Z.; Li, C.; Jia, M.; Shi, K.; Wen, Y.; Wang, W. Applicability Assessment of Stearic Acid/palmitic Acid Binary Eutectic Phase Change Material in Cooling Pavement. *Renew Energy* **2021**, 175, 748-759.
9. Yang, M.; Zhong, H.; Li, T.; Wu, B.; Wang, Z.; Sun, D. Phase Change Material Enhanced Radiative Cooler for Temperature-Adaptive Thermal Regulation. *ACS Nano.* **2023**, 17, 1693-1700.
10. Nižetić, S.; Jurčević, M.; Čoko, D.; Arıcı, M.; Hoang, A. T. Implementation of Phase Change Materials for Thermal Regulation of Photovoltaic Thermal Systems: Comprehensive Analysis of Design Approaches. *Energy* **2021**, 228, 120546.
11. Liang, S.; Xu, F.; Li, W.; Yang, W.; Cheng, S.; Yang, H.; Chen, J.; Yi, Z.; Jiang, P. Tunable Smart Mid Infrared Thermal Control Emitter Based on Phase Change Material VO_2 Thin Film. *Appl. Therm. Eng.* **2023**, 232, 121074.
12. Lawag, R. A.; Ali, H. M. Phase Change Materials for Thermal Management and Energy Storage: A Review. *J. Energy. Storage.* **2022**, 55, 105602.
13. Zhang, Z.; Zhang, Z.; Chang, T.; Wang, J.; Wang, X.; Zhou, G. Phase Change Material Microcapsules with Melamine Resin Shell *via* Cellulose Nanocrystal Stabilized Pickering Emulsion *In Situ* Polymerization. *Chem. Eng. J.* **2022**, 428, 131164.
14. Hassan, F.; Jamil, F.; Hussain, A.; Ali, H. M.; Janjua, M. M.; Khushnood, S.; Farhan, M.; Altaf, K.; Said, Z.; Li, C. Recent Advancements in Latent Heat Phase Change Materials and Their Applications for Thermal Energy Storage and Buildings: A State of the Art Review. *Sustain. Energy Technol. Assess.* **2022**, 49, 101646.
15. Soo, X. Y. D.; Png, Z. M.; Chua, M. H.; Yeo, J. C. C.; Ong, P. J.; Wang, S.; Wang, X.; Suwardi, A.; Cao, J.; Chen, Y.; Yan, Q.; Loh, X. J.; Xu, J.; Zhu, Q. A Highly Flexible Form-stable Silicone-octadecane PCM Composite for Heat Harvesting. *Mater. Today. Adv.* **2022**, 14, 100227.
16. Das, D.; Masek, O.; Paul, M. C. Development of Novel Form-stable PCM-biochar Composites and Detailed Characterization of Their Morphological, Chemical and Thermal Properties, *J. Energy. Storage* **2024**, 84, 110995.
17. Das, A.; Apu, M. M. H.; Akter, A.; Al Reza, M. M.; Mia, R. An Overview of Phase Change Materials, Their Production, and Applications in Textiles. *Results in Eng.* **2025**, 25, 103603.
18. Liang, C.; Zhang, W.; Liu, C.; He, J.; Xiang, Y.; Han, M.; Tong, Z.; Liu, Y. Multifunctional Phase Change Textiles with Electromagnetic Interference Shielding and Multiple Thermal Response Characteristics. *Chem. Eng. J.* **2023**, 471, 144500.
19. Hekimoğlu, G.; Sarı, A.; Arunachalam, S.; Arslanoğlu, H.; Gencel, O. Porous Biochar/heptadecane Composite Phase Change Material with Leak-proof, High Thermal Energy Storage Capacity and Enhanced Thermal Conductivity. *Powder Technol.* **2021**, 394, 1017-1025.
20. ce Gao, D.; Sun, Y.; Fong, A. M.; Gu, X. Mineral-based Form-stable Phase Change Materials for Thermal Energy Storage: A State-of-the Art Review. *Energy Storage Mater.* **2022**, 46, 100-128.
21. Ge, X.; Tay, G.; Hou, Y.; Zhao, Y.; Sugumaran, P. J.; Thai, B. Q.; Ang, C. K.; Zhai, W.; Yang, Y. Flexible and Leakage-proof Phase Change Composite for Microwave Attenuation and Thermal Management. *Carbon N.Y.* **2023**, 210, 118084.

Publisher's Note The Polymer Society of Korea remains neutral with regard to jurisdictional claims in published articles and institutional affiliations.